Target Identification

DOI: 10.1002/ange.201304987

Identification of Malate Dehydrogenase 2 as a Target Protein of the HIF-1 Inhibitor LW6 using Chemical Probes**

*Kyeong Lee, Hyun Seung Ban, Ravi Naik, Ye Seul Hong, Seohyun Son, Bo-Kyung Kim, Yan Xia, Kyung Bin Song, Hong-Sub Lee, and Misun Won**

Hypoxia-inducible factor (HIF) regulates tumor angiogenesis and metastasis in response to low oxygen tension.[1] In the presence of oxygen, HIF-1α is rapidly degraded through the ubiquitin–proteasome pathway. In hypoxic conditions, stabilized HIF-1α dimerizes with HIF-1β. The HIF-1α/β heterodimer binds to hypoxia response elements (HRE) in gene promoters and induces the expression of target genes involved in angiogenesis, metastasis, glycolysis, cell proliferation, and resistance to apoptosis.[2] Increased expression of HIF-1α in many solid tumors correlates with aggressive tumor growth, therapeutic resistance, and a poor clinical outcome. HIF-1α shifts the metabolism from oxidative phosphorylation to anaerobic glycolysis.[3] Therefore, HIF-1α is an important therapeutic target for cancer.

We previously synthesized and evaluated aryloxyacetylamino benzoic acid analogues.[4] LW6 (**1** in Figure 1A) potently inhibited HIF-1α accumulation by degrading HIF-1α without affecting the HIF-1α mRNA levels during hypoxia.[4a,b] LW6, which is commercially available, has been used in various studies as an HIF-1α inhibitor.[5] However, the molecular target of LW6 remains unknown.

To identify a drug target, chemical biological methods such as activity-based probes (ABPs),[6] photoaffinity labeling, biotinylation, and click conjugation have been used.[7] Herein, we identify the molecular target of **1** using chemical probes. Cellular images and direct protein interactions of **1** were examined in living cells with a series of chemical probes (**2**–**6**), which were designed using the structure–activity relationship (SAR) of **1**.[4a] Synthesis and characterization data for these probes are available in the Supporting Information.

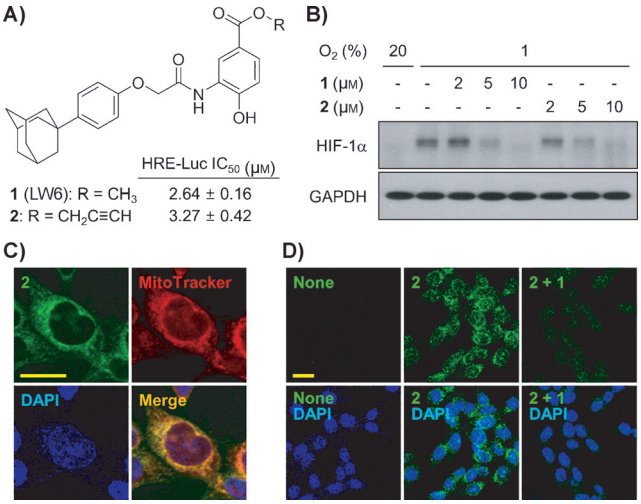

Figure 1. Biological activities and cellular localization of a chemical probe for LW6. A) Formula of **1** and its clickable probe **2**. B) Inhibitory effects of **1** and probe **2** on HIF-1α accumulation were determined by immunoblot analysis. C) Localization of probe **2** (3 μM, green) was detected through a click reaction using azide-linked Alexa Fluor 488 in HCT116 cells. Mitochondria were selectively stained with the MitoTracker probe (red). Nuclei (blue) were stained with 4,6-diamidino-2-phenylindole (DAPI). D) Competitive binding of probe **2** (3 μM) to its target molecules in the presence or absence of **1** (10 μM). Scale bars = 20 μm.

The distribution of drug molecules within subcellular compartments can provide information about the mechanism of drug action. The intracellular localization of LW6 was visualized through click chemistry with probe **2**, containing an acetylene group, in colon cancer HCT116 cells (Figure 1A). Both **1** and **2** suppressed HIF-1α accumulation (Figure 1B) and HRE-luciferase activity (Figure 1A; Supporting Information, Figure S12). Subsequently, the cellular localization of probe **2** was determined by a click reaction with an azide-linked Alexa Fluor 488 molecule. Notably, copper-catalyzed azide–alkyne cycloadditions (click reactions) are highly specific and efficient bio-orthogonal reactions[7b] to visualize intracellular probe distribution. We found that compound **2** was localized primarily in the cytoplasm (Figure 1C). The co-localization of compound **2** (3 μM) with the mitochondria-selective probe, MitoTracker (500 nM), indicated that **2** is specifically localized in the mitochondria, whereas the localization of an adamantyl-free probe **4** was not observed (Figure S13). The mitochondrial localization of probe **2** was

[*] Dr. H. S. Ban,[+] Y. S. Hong, Dr. B.-K. Kim, Dr. M. Won
Medical Genomics Research Center, Korea Research Institute of Bioscience and Biotechnology
125 Gwahak-ro, Yuseong-gu, Daejeon 305-806 (Korea)
E-mail: misun@kribb.re.kr
Prof. K. Lee,[+] R. Naik, S. Son, Dr. Y. Xia
College of Pharmacy, Dongguk University-Seoul
26 Pildong, Junggu, Seoul 100-715 (Korea)
Prof. K. B. Song
Department of Food Science and Technology
Chungnam National University
99 Daehak-ro, Yuseong-gu, Daejeon 305-764 (Korea)
Dr. H.-S. Lee
ILDONG Pharmaceutical Co. Ltd.
23-9 Seogwoo-dong, Hwaseong, Kyungi-do 445-811 (Korea)
[+] These authors contributed equally to this work.
[**] This work was supported in part by the KRIBB Initiative Program, NRF-2011-0031690, and NRF-2012M3A9C1053532.
Supporting information for this article is available on the WWW under http://dx.doi.org/10.1002/anie.201304987.

attenuated by competition from unlabeled **1** (10 μM) (Figure 1D), confirming that **1** also localizes in the mitochondria.

Mitochondrial respiration consumes cellular oxygen and controls intracellular oxygen tension through the electron transport chain (ETC). Pharmacological inhibition of mitochondrial respiration increases intracellular oxygen concentrations, inducing degradation of HIF-1α.[8] The mitochondrial localization of probe **2** suggests that **1** may inhibit mitochondrial respiration. Accordingly, we examined the effects of **1** on cellular oxygen consumption with an XF24 Extracellular Flux Analyzer. Real-time oxygen consumption rates (OCR) for the basal and maximal respirations were determined in the presence of **1** (Figure 2A). The basal and maximal respirations were measured by treatment with oligomycin, the ATP synthase inhibitor, and trifluorocarbonylcyanide phenylhydrazone (FCCP), which decouples ATP synthesis, respectively. As a result, OCR and total oxygen consumption were inhibited by **1** in a concentration-dependent manner during respiration (Figure 2A,B). Cellular ATP production was reduced by **1**, presumably because respiration was inhibited (Figure S14). These results suggest that **1** promotes HIF-1α degradation by reducing the mitochondrial oxygen consumption and increasing the intracellular oxygen during hypoxia.

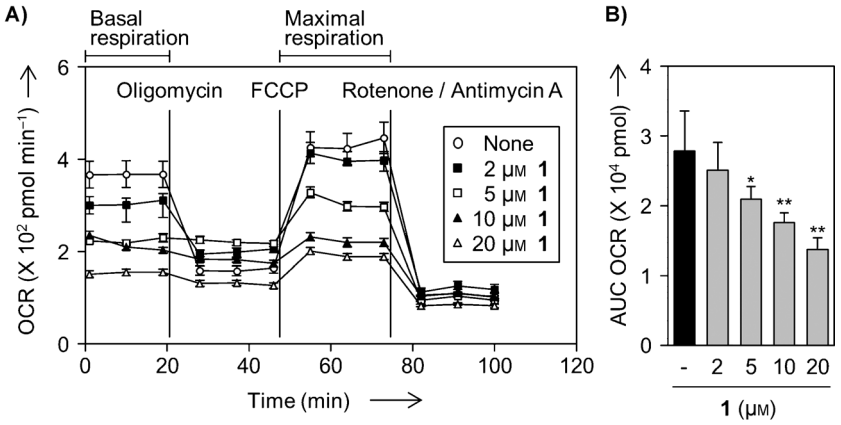

Figure 2. Inhibition of mitochondrial respiration by **1**. A) OCR was determined at the indicated concentrations of **1** in HCT116 cells. The basal and maximal OCR were measured by adding oligomycin (1 μM), FCCP (0.5 μM), and rotenone (1 μM)/antimycin A (1 μM). B) The total oxygen consumption was determined by calculating the area under the curve (AUC). Values represent the mean of three samples. Vertical bars indicate standard deviation (S.D.). Statistical significance: $*P<0.05$, $**P<0.01$; compared to untreated control cells.

Subsequently, we added trifluoromethyl diazirine to probe **2**, generating the photoactivatable probe **3** (Figure 3A). Trifluoromethyl diazirine has several valuable characteristics, including photoactivity at long wavelengths, good chemical stability, rapid photolysis, and generation of a highly reactive carbene.[9] A cell-based HRE reporter assay and immunoblot analysis demonstrated that probe **3** (10 μM) suppressed hypoxia-induced HIF-1α accumulation, while the adamantyl-free probe **4** (10 μM), a negative control, did not (Figure 3B).

Photoaffinity labeling was performed in the HCT116 cells using ultraviolet irradiation and click conjugation with a fluorescent dye (Cy5 for probe **3** and Cy3 for probe **4**). Cellular proteins were separated by sodium dodecyl sulfate-polyacrylamide gel electrophoresis (SDS-PAGE) and visualized by in-gel fluorescence scanning. A Cy5-specific band was detected at 30–37 kDa (Figure 3C). Competition between probes **3** and **1** reduced the Cy5 fluorescence intensity (Figure 3D).

Two-dimensional gel electrophoresis (2DE) was performed to separate the proteins bound to probes **3** and **4** (Figure 4; Figure S18), followed by in-gel trypsin digestion and mass spectrometry. We expected that the protein specifically bound to probe **3**–Cy5 would appear red in an overlaid gel and be localized to the mitochondria. From an analysis of the red fluorescence, malate dehydrogenase 2 (MDH2) was identified as a protein bound to probe **3**–Cy5 (Table S1). MDH2 is a 36 kDa mitochondrial enzyme that catalyzes the malate/NAD^+ conversion to oxaloacetate/

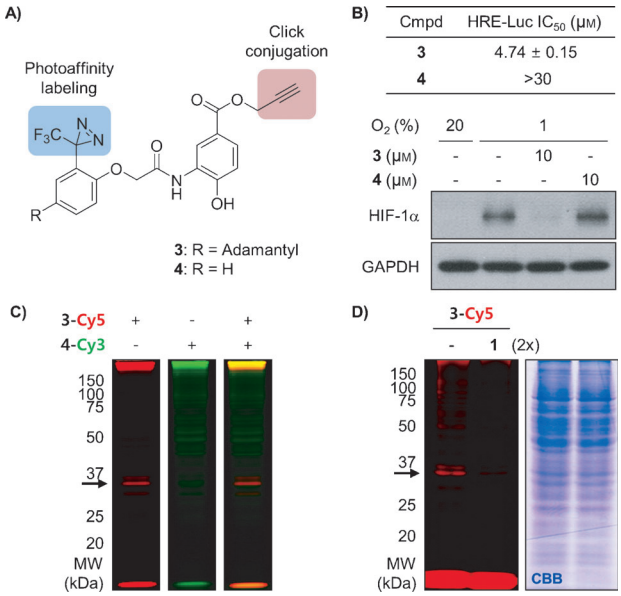

Figure 3. Target identification with multifunctional chemical probes. A) Multifunctional chemical probes for photoaffinity labeling and click conjugation. B) Effects of the probes on transcriptional activity (HRE-Luc) and accumulation of HIF-1α. C) Proteins conjugated to probe **3**–Cy5 (50 μM) or probe **4**–Cy3 (50 μM) were detected by in-gel fluorescence after SDS-PAGE. D) Competitive binding of probe **3**–Cy5 to the target protein in the presence of **1** (100 μM). Coomassie brilliant blue (CBB) staining of the gel is shown.

NADH during the tricarboxylic acid cycle (TCA cycle) and functions as a respiratory substrate in the mitochondrial ETC.[10]

To confirm the binding of **1** to MDH2, biotin affinity probes were synthesized (Figure 5A). In the affinity pull-down assays, MDH2 bound to biotinylated **1** (**6**), compared with a negative control the adamantyl-free biotinylated probe (**5**; Figure 5B). Binding of biotinylated **1** to MDH2 was

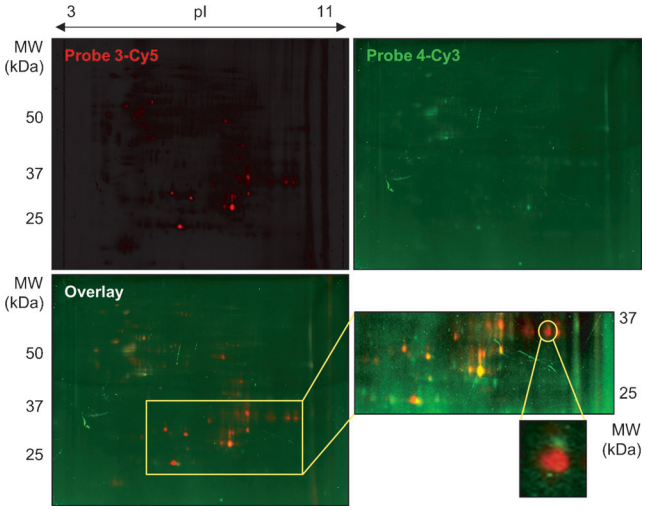

Figure 4. Two-dimensional electrophoresis and imaging. Photoaffinity labeling of cellular proteins was followed by click conjugation with a fluorescent dye (Cy5 for probe **3** and Cy3 for probe **4**). The cellular proteins conjugated to probe **3**–Cy5 or probe **4**–Cy3 were separated by two-dimensional electrophoresis and visualized by in-gel fluorescence scanning.

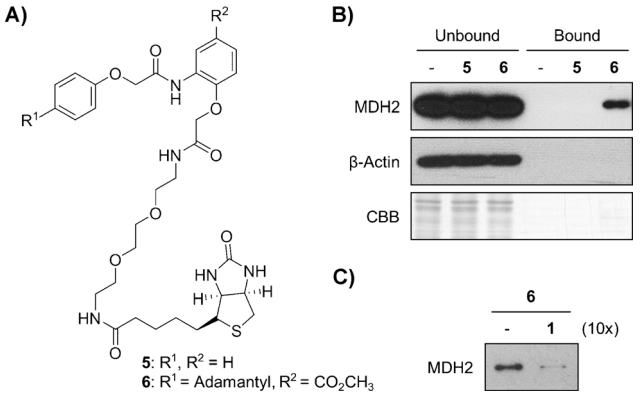

Figure 5. Pull-down assay of the biotinylated probes. A) Formula of the biotinylated probes. B) Affinity pull-down assay. HCT116 cell lysates were incubated with biotinylated probe (5 μM) and avidin resin. MDH2 was detected by immunoblot analysis after SDS-PAGE. C) Competition assay. The binding of MDH2 to biotinylated probe **6** (5 μM) was inhibited by the presence of **1** (50 μM).

attenuated by addition of non-biotinylated **1** (Figure 5C). These results clearly support an interaction between **1** and MDH2.

In addition, fluorescent probe **3** bound to purified recombinant human MDH2 (rh-MDH2; Figure 6A, middle lane) and its binding was reduced in the presence of **1** (right lane), indicating that probe **3** bound directly to MDH2. Next, we examined the effect of **1** and probes on the MDH2 activity using MDH2 isolated from HCT116 cells. We found that **1** and **3**, but not **4**, inhibited the MDH2 activity in a concentration-dependent manner (Figure 6B; Figure S15) without affecting the MDH2 expression (Figure S16). Then, we found the MDH2 inhibitor L-thyroxine **7**[11] (Figure 6C) inhibited transcriptional activity (HRE-Luc $IC_{50} = 26.3 \pm 0.97$ μM; Figure S17) and accumulation (Figure 6D) of HIF-1α. However, **1** (20 μM) demonstrated a much stronger effect on MDH2 inhibition (Figure 6B) and oxygen consumption than **7** (80 μM; Figure 6E). Thus, we suggest that LW6 binds to MDH2 to block the TCA cycle, thereby inhibiting mitochondrial respiration and increasing the local oxygen tension. This result explains our previous finding that **1** promotes HIF-1α degradation through proteasome-dependent degradation.[4b] This is the first report that MDH2 regulates HIF-1α accumulation under hypoxia.

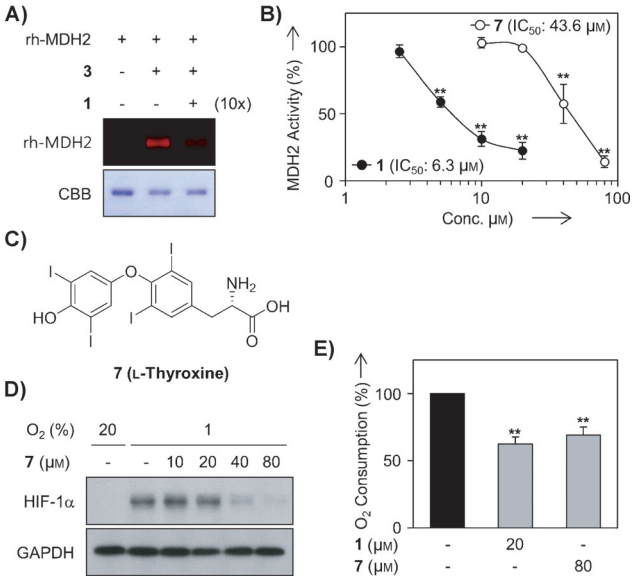

Figure 6. Inhibition of MDH2 activity by **1** and **7**. A) In vitro binding of **3** (10 μM) to human recombinant MDH2 and competition assay with **1** (100 μM). B) Effects of **1** and **7** on the activity of isolated MDH2 from HCT116 cells. C) Formula of L-thyroxine (**7**). D) Inhibition of HIF-1α accumulation by **7**. E) Inhibition of oxygen consumption by **1** (20 μM) and **7** (80 μM) in HCT116 cells. Values are the mean averages of three samples, vertical bars indicate S.D. $^{**}P < 0.01$, compared with untreated control cells.

A high level of MDH2 expression was associated with shorter, relapse-free survival and chemoresistance of prostate cancer patients.[12] The knockdown of MDH2 enhanced docetaxel sensitivity and induced metabolic inefficiency. Future studies should examine the relevance of MDH2 with respect to HIF-1 regulation in cancer and the potential benefits of MDH2 inhibition with cancer therapeutics.

Our chances of isolating MDH2 as a target of **1** were improved by using a photoactivatable trifluoromethyl diazirine and a fluorescent probe in living cells. These modifications overcame the common limitations of conventional methods (e.g., poor detection or low affinity of target molecules). Nonspecific binding proteins were excluded by double fluorescent labeling and 2DE.

In summary, we designed and synthesized a series of LW6 (**1**)-derived chemical probes by installing a clickable tag and a photoactivatable moiety. We observed the mitochondrial localization of **1** and identified MDH2 as a target protein. In parallel with the MDH2 inhibition, **1** and MDH2 inhibitor **7** suppressed hypoxia-induced HIF-1α accumulation by inhibiting mitochondrial respiration. In conclusion, LW6 reduces

HIF-1α accumulation by inhibiting MDH2 activity and suppressing mitochondrial respiration.

Received: June 10, 2013
Published online: August 9, 2013

Keywords: click chemistry · fluorescent probes · HIF inhibitors · malate dehydrogenase 2 · photoaffinity labeling

[1] G. L. Wang, B. H. Jiang, E. A. Rue, G. L. Semenza, *Proc. Natl. Acad. Sci. USA* **1995**, *92*, 5510 – 5514.
[2] G. L. Semenza, *Nat. Rev. Cancer* **2003**, *3*, 721 – 732.
[3] G. L. Semenza, *Curr. Opin. Genet. Dev.* **2010**, *20*, 51 – 56.
[4] a) K. Lee, J. H. Lee, S. K. Boovanahalli, Y. Jin, M. Lee, X. Jin, J. H. Kim, Y. S. Hong, J. J. Lee, *J. Med. Chem.* **2007**, *50*, 1675 – 1684; b) K. Lee, J. E. Kang, S. K. Park, Y. Jin, K. S. Chung, H. M. Kim, K. Lee, M. R. Kang, M. K. Lee, K. B. Song, E. G. Yang, J. J. Lee, M. Won, *Biochem. Pharmacol.* **2010**, *80*, 982 – 989; c) R. Naik, M. Won, B. K. Kim, Y. Xia, H. K. Choi, G. Jin, Y. Jung, H. M. Kim, K. Lee, *J. Med. Chem.* **2012**, *55*, 10564 – 10571.
[5] a) Y. Hashimoto, H. Tazawa, F. Teraishi, T. Kojima, Y. Watanabe, F. Uno, S. Yano, Y. Urata, S. Kagawa, T. Fujiwara, *PLoS One* **2012**, *7*, e39292; b) L. Wang, Y. O. Son, S. Ding, X. Wang, J. A. Hitron, A. Budhraja, J. C. Lee, Q. Lin, P. Poyil, Z. Zhang, J. Luo, X. Shi, *Toxicol. Sci.* **2012**, *130*, 269 – 280.
[6] a) J. Park, M. Koh, S. B. Park, *Mol. Biosyst.* **2013**, *9*, 544 – 550; b) U. Rix, G. Superti-Furga, *Nat. Chem. Biol.* **2009**, *5*, 616 – 624; c) M. Schenone, V. Dancik, B. K. Wagner, P. A. Clemons, *Nat. Chem. Biol.* **2013**, *9*, 232 – 240.
[7] a) F. Kotzyba-Hibert, I. Kapfer, M. Goeldner, *Angew. Chem.* **1995**, *107*, 1391 – 1408; *Angew. Chem. Int. Ed. Engl.* **1995**, *34*, 1296 – 1312; b) H. C. Kolb, M. G. Finn, K. B. Sharpless, *Angew. Chem.* **2001**, *113*, 2056 – 2075; *Angew. Chem. Int. Ed.* **2001**, *40*, 2004 – 2021; c) V. V. Rostovtsev, L. G. Green, V. V. Fokin, K. B. Sharpless, *Angew. Chem.* **2002**, *114*, 2708 – 2711; *Angew. Chem. Int. Ed.* **2002**, *41*, 2596 – 2599.
[8] Y. Chua, E. Dufour, E. Dassa, P. Rustin, H. Jacobs, C. Taylor, T. Hagen, *J. Biol. Chem.* **2010**, *285*, 31277 – 31284.
[9] M. Hashimoto, Y. Hatanaka, *Eur. J. Org. Chem.* **2008**, 2513 – 2523.
[10] C. R. Goward, D. J. Nicholls, *Protein Sci.* **1994**, *3*, 1883 – 1888.
[11] S. Varrone, E. Consiglio, I. Covelli, *Eur. J. Biochem.* **1970**, *13*, 305 – 312.
[12] Q. Liu, C. T. Harvey, H. Geng, C. Xue, V. Chen, T. M. Beer, D. Z. Qian, *Prostate* **2013**, *73*, 1028 – 1037.